Chemical Science

ROYAL SOCIETY OF CHEMISTRY

EDGE ARTICLE

View Article Online
View Journal | View Issue

Cite this: *Chem. Sci.*, 2024, **15**, 20030

All publication charges for this article have been paid for by the Royal Society of Chemistry

Received 24th September 2024
Accepted 9th November 2024

DOI: 10.1039/d4sc06462c

rsc.li/chemical-science

Diphosphaenones: beyond the phosphorus analogue of enones†

Jieli Lin, Shihua Liu, Shunlin Zheng, Hansjörg Grützmacher, Cheng-Yong Su and Zhongshu Li *

Phosphaenones, like their carbon analogue enones (C=C–C=O), are promising building blocks for synthetic chemistry and materials science. However, in contrast to the α- and β-phosphaenones, structurally and spectroscopically well-defined diphosphaenones (DPEs) are rare. In this study, we disclose the isolation and spectroscopic characterization of N-heterocyclic vinyl (NHV) substituted acyclic DPEs **3a,b** [NHV–P=P–C(O)–NHV]. X-ray diffraction methods allowed determination of the structures, which show a central planar *trans* P=P–C=O configuration. Compound **3a** behaves like classical enones and shows 1,4-addition across the P=P–C=O unit, which proceeds in a stepwise manner. In contrast, **3a** exhibits also 1,2-addition across the P=P but not the C=O double bond, which differentiates it from enones.

Introduction

The diagonal relationship between carbon and phosphorus has not only inspired the synthesis of organophosphorus compounds but also expanded our understanding of molecular properties on one side and the limits of concepts based on analogies on the other.[1] Phosphabenzenes, phosphaalkenes, phosphaalkynes, diphosphenes, and other related compounds closely mimic their carbon analogues while also exhibiting distinctive electronic properties due to the incorporation of heavier elements.[2] These compounds became valuable building blocks in synthetic chemistry and materials science and like their carbon counterparts allow to synthesize organophosphorus compounds in an especially efficient and frequently atom-economic way.[3] This is also true for enones [R_2C=CR–C(O)R], which represent a widely investigated class of compounds in classical organic syntheses.[4] By replacing one or two CR groups of enones with P atoms, α-phosphaenones [α-PEs, R_2C=P–C(O)R], β-phosphaenones [β-PEs, RP=CR–C(O)R], and diphosphaenones [DPEs, RP=P–C(O)R] can be engineered (Fig. 1a).

The synthesis of stable α-PEs (**I**, Fig. 1) was initially achieved by M. Regitz and co-workers through the nucleophilic attack from P-silyl-substituted phosphaalkene [R_2C=P–$SiMe_3$] to acyl chlorides.[5] The first stable β-PEs (**II**, Fig. 1) were independently reported by the groups of F. Bickelhaupt[6] and M. Yoshifuji[7] through nucleophilic attack of a carbenoid phosphanylidene [Mes*P=C(Cl)Li] to acyl chlorides. Other stable β-PEs were also successfully prepared using cyclic rigid frameworks.[8] However,

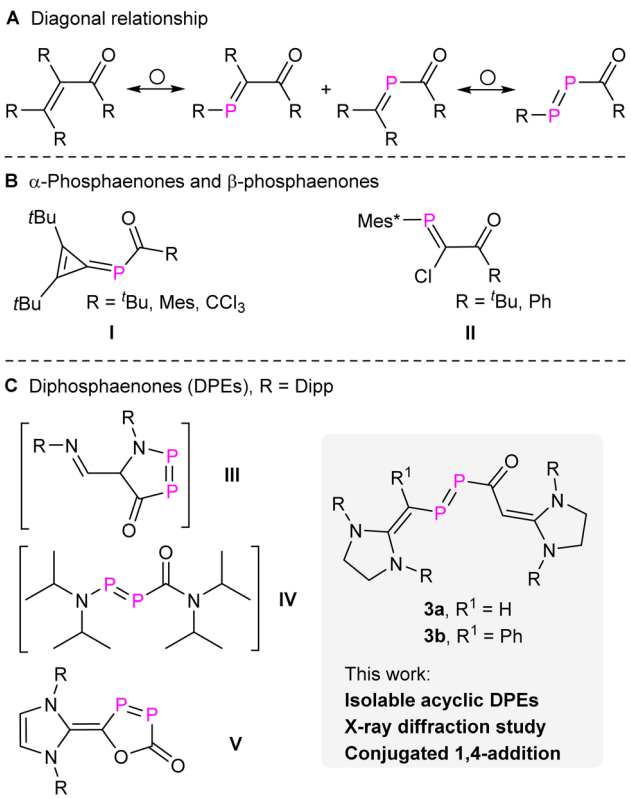

Fig. 1 (A) Diagonal relationship between enones and their phosphorus analogues. (B and C) Selected examples of α-phosphaenones, β-phosphaenones, and diphosphaenones. Mes, 2,4,6-tri-methylphenyl; Mes*, 2,4,6-tri-*tert*butylphenyl; Dipp, 2,6-di-isopropylphenyl.

LIFM, IGCME, School of Chemistry, Sun Yat-Sen University, Guangzhou 510006, China. E-mail: lizhsh6@mail.sysu.edu.cn

† Electronic supplementary information (ESI) available: Synthesis and characterization of compounds, NMR spectra, crystallographic, and computational details. CCDC 2343829, 2343830, 2343833–2343835, 2346470, and 2385608. For ESI and crystallographic data in CIF or other electronic format see DOI: **https://doi.org/10.1039/d4sc06462c**

the synthesis and isolation of DPEs remains challenging. Previously, we proposed the presence of two transient DPEs, the first cyclic (**III**, Fig. 1)[9] and acyclic DPEs (**IV**, Fig. 1),[10] which were confirmed through trapping experiments *via* the [2 + 4] or [2 + 2] cycloaddition across the P═P double bond. Seminal work from the group of Protasiewicz revealed the first stable cyclic DPE (**V**, Fig. 1)[11] through the treatment of [(NHC–Cl)Cl] (NHC═N-heterocyclic carbene) with two equivalents of sodium phosphaethynolate [Na(OCP)].[12] However, stable acyclic DPEs remain elusive to date.

In the present work, we report the synthesis of N-heterocyclic vinyl (NHV)[13] substituted compounds **3a,b** [NHV–P═P–C(O)–NHV] (Fig. 1). The characterization of **3a,b** as DPEs is strongly supported by X-ray crystal diffraction (XRD) studies, multinuclear NMR spectra analyses, and quantum chemical calculations. In addition, **3a** behaves like enones showing 1,4-additions in a stepwise manner, which differentiates it from classical diphosphenes. To date only one example among PEs, a cyclic *cis* β-PE, has been reported to undergo likewise a conjugated 1,4-addition.[8e] The replacement of both CR with P atoms in enones alters more profoundly the electronic structure and indeed, **3a** exhibits also 1,2-addition across the P═P double bond, but not the C═O double bond.

Results and discussion

Synthesis and characterization of DPEs 3a,b

The NHV substituted[14] phosphenium chloride **1a** (R═H) and **1b** (R═Ph) ([L═C(R)–P–CH═L)$^+$Cl$^-$], L = **SIPr** = (1,3-bis-(2,6-diisopropylphenyl)imidazolidin-2-ylidine) were prepared as orange powders [**1a**: $\delta(^{31}P)$ = 331.7 ppm]; **1b**: $\delta(^{31}P)$ = 323.3 ppm; see ESI† for further details). Treatment of **1a,b** with an equimolar amount of Na(OCP) exclusively afforded **3a,b** (L═C(R)–P═P–C(O)–C(H)═L, **3a**: R═H; **3b**: R═Ph) as red powders in more than 74% yield under the elimination of sodium chloride (Fig. 2A). The formation of **3a,b** is likely to occur through the intramolecular rearrangement of transient phosphanyl phosphaketenes **2a,b** ([NHV–P(P═C═O)–NHV]).[10] Both **3a,b** are stable in the solid state under a nitrogen atmosphere for weeks without noticeable decomposition, but they are highly sensitive to air and moisture. Additionally, no apparent decomposition or isomerization products were detected after irradiating a toluene solution of **3a,b** with LED light at 455 or 520 nm at 0 °C for 30 minutes.[14d] But **3a** slowly dimerizes in solution *via* the [2 + 2] cycloaddition across the P═P double bond.[15] Similar dimerization process was not observed for **3b**, likely due to the presence of additional phenyl substituents. After storing the saturated hexane solution of **3a** at room temperature under an inert atmosphere *via* slow evaporation for one-week, yellow crystalline product as the dimer of **3a** precipitated in 61% yield. The multinuclear NMR spectra analyses (Fig. S14–18†) and XRD study (Fig. S120†) confirmed that the dimerization proceeds in a highly regioselective manner affording thermodynamically favorable head to head dimer (Fig. S129†).[15]

Red single crystals of **3a,b** were grown from saturated hexane solutions at −30 °C and studied by XRD analyses (Fig. 2B). In the case of **3a**, the central P═P–C═O fragment is almost planar

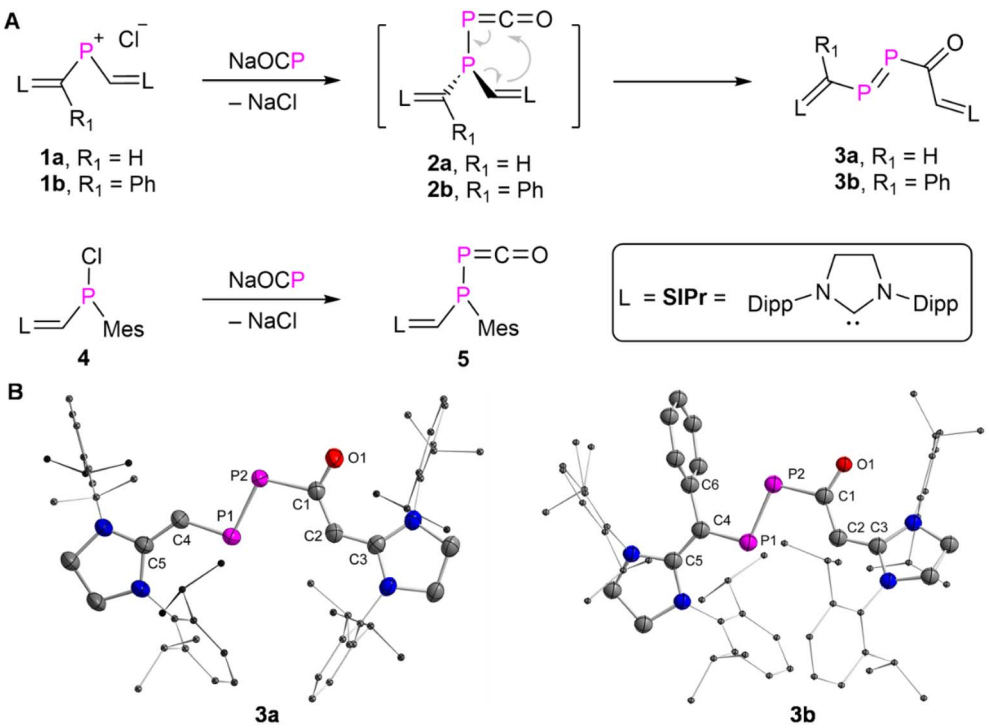

Fig. 2 (A) Synthesis of **3**–**5**. (B) Solid-state structure of **3a** and **3b** (ellipsoids are set to 50% probability; H atoms are omitted for clarity). Selected distances (Å): **3a**: P1–P2 2.0609(7), P2–C1 1.874(19), C1–O1 1.242(2), C1–C2 1.416(3), C2–C3 1.385(3), P1–C4 1.749(2), C4–C5 1.389(3); **3b**: P1–P2 2.0657(19), P2–C1 1.861(6), C1–O1 1.220(6), C1–C2 1.454(7), C2–C3 1.376(7), P1–C4 1.762(6), C4–C5 1.391(7), C4–C6 1.500(7).

[∠P1P2C1O1 = 173.26(13)°], and coplanar with the two terminal NHV moieties [∠C5C4P1P2 = 170.1(2)°, ∠P2C1C2C3 = 174.03(16)°]. This indicates the presence of electron delocalization across the NHV–P–P–C(O)–NHV skeleton. The delocalized double bonds C5=C4 [1.389(3) Å], P1=P2 [2.0609(7) Å], C1=O1 [1.242(2) Å], and C2=C3 [1.385(3) Å] are connected *via* single bonds C4–P1 [1.749(2) Å], P2–C1 [1.874(19) Å], and C1–C2 [1.416(3) Å] [Σr_{cov}(P–C) = 1.86 Å, Σr_{cov}(P=C) = 1.69 Å, Σr_{cov}(C–C) = 1.50 Å, Σr_{cov}(C=C) = 1.34 Å, Σr_{cov}(C–O) = 1.38 Å, Σr_{cov}(C=O) = 1.24 Å],[16] respectively. The P2–C1 bond is longer than that of the C4–P1 bond, which is likely due to hyperconjugation n(O1) → σ*(P2–C1).[17] **3b** exhibits similar structural metrics to those of **3a**, but with an additional phenyl substituent at C4 (C4–C6 [1.500(7) Å]).

Natural bond orbital (NBO) calculations[18] allow a more detailed insight into the bonding scenario of a simplified model $\mathbf{3a^M}$, where the NHC **SIPr** was replaced with **SIMe** (1,3-dimethylimidazoline-2-ylidine) (Fig. S121†). An inspection of the Wiberg bond indices (WBIs) of $\mathbf{3a^M}$ suggested that the WBIs of alternating double [C5=C4 (1.51), P1=P2 (1.75), C1=O1 (1.64), and C2=C3 (1.40)] and single [C4–P1 (1.10) and C1–C2 (1.20)] bonds are substantially smaller or larger than expected, respectively. Only single bond P2–C1 (0.93) for which the bond order turned to be even smaller. Second-order perturbation theory analyses revealed the donor–acceptor energies $E(2)$ for the delocalization of the lone pair localized on the O1 to σ*(P2–C1) is 29.86 kcal mol^{-1}, which is larger than the donation into σ*(C1–C2) (22.60 kcal mol^{-1}). The strength of the π-type interaction, including both electron-donation and acception between the central double bonds of $\mathbf{3a^M}$, follows the order: 49.75 kcal mol^{-1} (C1=O1 ↔ C2=C3) > 23.63 kcal mol^{-1} (P1=P2 ↔ C4=C5) > 10.65 kcal mol^{-1} (C1=O1 ↔ P1=P2). Thus, NBO calculations support the presence of significant hyperconjugation n(O1) → σ*(P2–C1) and π-type electron delocalization within the P=P–C=O moiety, which aligns with the relatively long P2–C1 bond and nearly planar P=P–C=O configuration (see XRD analyses).

The proton-decoupled ^{31}P NMR spectra of **3a** and **3b** show two characteristic doublets at $\delta(^{31}P)$ = 487.5 (P1) and 385.0 ppm (P2, $^1J_{PP}$ = 529.5 Hz), and $\delta(^{31}P)$ = 525.9 (P1) and 376.7 ppm (P2, $^1J_{PP}$ = 515.9 Hz), respectively. The chemical shift assignment was made by comparison with the calculated chemical shifts [$\mathbf{3a^M}$: 511.3 (P1) and 413.9 ppm (P2), Table S2†].[19] The large $^1J_{PP}$ coupling constants are indicative of the presence of a P=P double bond in both **3a,b**.[3h,15] In the ^{1}H NMR spectra, a broad singlet at 5.77 ppm due to the small and unresolved $^2J_{PH}$ coupling, and a sharp singlet at 4.77 ppm were attributed to the protons of the C4–H and C2–H at the NHV moieties for **3a**. A sharp singlet at 4.54 ppm is assigned to the proton of C2–H and characterizes **3b**, which shows no further resonances between 4.0–6.5 ppm. The proton-decoupled ^{13}C NMR spectra displayed high-frequency shifted multiplets assigned to the carbonyl group at 198.9 ppm and 198.3 ppm for **3a** and **3b**, respectively. Solutions of **3a** and **3b** in toluene are red and exhibit strong absorptions at λ_{max} = 488 nm (5.0 × 10^4 M^{-1} cm^{-1}) and 496 nm (2.0 × 10^4 M^{-1} cm^{-1}), respectively. According to time-dependent density functional theory (TD-DFT) calculations, these absorptions arise from electronic transitions of the highest occupied molecular orbital (HOMO) to the lowest unoccupied molecular orbital (LUMO) (π–π*, Fig. S90 and S91†).

Chlorophosphine **4** [$\delta(^{31}P)$ = 96.3 ppm] with NHV and 2,4,6-tri-methylphenyl substituents was prepared as a white powder in 90% yield (see ESI† for details). Treatment of **4** with an equimolar amount of Na(OCP) provided exclusively the phosphanyl phosphaketene **5** [$\delta(^{31}P)$ = −41.0 and −248.6 ppm, $^1J_{PP}$ = 170.9 Hz] as white powder in 55% yield (Fig. 2).[9,20] In solution at room temperature, **5** did not convert to the DPE but decomposed into an unidentified mixture (Fig. S39†).

To gain a deeper understanding of a possible mechanism leading to **3a,b**, DFT calculations were carried out for the rearrangement of the simplified model $\mathbf{2b^M}$ at the M062X/Def2TZVP-SMD(toluene)//M062X/Def2SVP level of theory.[21] The minimum energy reaction pathways (MERPs) for two possible rearrangements are shown in Fig. 3A. The rearrangement starts with a nucleophilic attack of the parent or phenyl substituted NHV on the electron-deficient carbon of the PCO moiety *via* the activated complex **TS1-b** (14.2 kcal mol^{-1}) or **TS1-c** (17.1 kcal mol^{-1}). Subsequently, the four-membered heterocycles **IN1-b** (10.5 kcal mol^{-1}) or **IN1-c** (6.9 kcal mol^{-1}) are formed in an endothermic reaction. A subsequent P–C cleavage is easily achieved *via* **TS2-b** (9.0 kcal mol^{-1}) or **TS2-c** (6.4 kcal mol^{-1}) to generate kinetically and thermodynamically favourable products $\mathbf{3b^M}$ (−7.9 kcal mol^{-1}) or $\mathbf{3c^M}$ (−12.9 kcal mol^{-1}). Natural population analyses (NPA) charges were obtained from a NBO analysis[18] and indicate that the carbon of the PCO moiety is positively charged (+0.31*e*), whereas the vinyl carbons from the two NHV substituents are negatively charged. Specifically, the vinyl carbon (−0.80*e*) in the parent NHV possesses more electron density than the one with phenyl substituted NHV

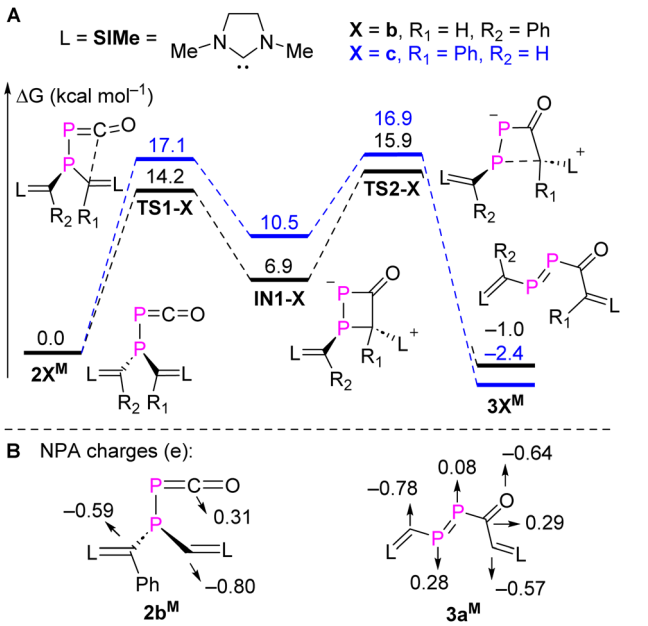

Fig. 3 (A) MERPs of the selective intramolecular rearrangement of $\mathbf{2b^M}$, and (B) selected NPA charges of $\mathbf{2b^M}$ and $\mathbf{3a^M}$ at M062X/Def2-TZVP-SMD(toluene)//M062X/Def2SVP level of theory.

moiety (−0.59*e*; Fig. 3B). The exergonic rearrangement from **2b^{M}** to **3b^{M}** is kinetically favoured by 2.9 kcal mol^{-1} over the formation of **3c^{M}**, which is in consistent with our experimentally observation that only **3b** was formed.

A detailed MO analysis at the M062X/Def2SVP level of theory provided insights into the electronic structure between **3a^{M}** and its hypothetical carbon analogue **B**, parent DPE **A** and parent enone **C** (Fig. 4). For the parent DPE **A**, the LUMO and HOMO-1 are primarily the π*-type and π-type orbitals of the P=P unit. The HOMO corresponds mainly the lone-pair type orbital derived from phosphorus and oxygen atoms. The HOMO and HOMO-1 of the parent enone **C** are also mainly combinations of the lone-pair type orbital from oxygen and π-type orbitals of the C=C unit. But the LUMO of **C** is the π*-type orbitals of the conjugated C=C–C=O. These frontier orbitals in **A** and **C** are seen in the NHV substituted derivatives **3a^{M}** and **B** as LUMO, HOMO, and HOMO-2. The strong electron releasing substituent NHV raises the energy levels of all orbitals discussed so far. The energy levels of the π-type orbitals (HOMO) are even higher than that of the combination of lone-pair type orbitals at O and both P (HOMO-2) in **3a^{M}** and **B** due to the strong π-electron delocalization over the NHV groups. Both HOMO-1 of **3a^{M}** and **B** are mainly attributed to the π-type bonding of one NHV group with a minor polarization towards the carbonyl group. Consequently, both **3a^{M}** and **B** are best viewed as NHV substituted DPE and enone.

Stepwise nucleophilic and electrophilic 1,4-addition (P,O) of 3a

As the phosphorus analogues of enones, DPEs are expected to exhibit also 1,4-addition reactivity over the P=P–C=O moiety. To probe this, we first treated **3a** with relatively weak nucleophiles such as an equivalent of either potassium bis(trimethylsilyl)amide [KN(TMS)$_2$] or potassium *tert*-butoxide [KO^{t}Bu] in tetrahydrofuran as solvent at room temperature. This resulted in nearly quantitative conversion to **6a** or **6b**, which were obtained as yellow powders in over 90% yield (Fig. 5A). The proton-decoupled ^{31}P NMR spectra of **6a** or **6b** displayed two doublets at $\delta(^{31}P) = 61.6$ and 29.7 ppm ($^{1}J_{PP} = 276.8$ Hz) or $\delta(^{31}P) = 104.9$ and 82.1 ppm ($^{1}J_{PP} = 301.8$ Hz), suggesting the conversion of the P=P π-bond into single bonds during the addition process. Reactions of **3a** with smaller or stronger nucleophiles, such as sodium methoxide, phenylmagnesium bromide or different hydride sources, led to rapid conversion of the **3a** but mixtures of unidentified products were obtained.

Single crystals of **6a** suitable for XRD analysis were obtained from a fluorobenzene solution layered with hexane and stored at −30 °C. The XRD study of **6a** unambiguously confirms the formation of a new P1–N1 single bond [1.7716(13) Å; Σr_{cov}(P–N) = 1.82 Å, Σr_{cov}(P=N) = 1.62 Å],[16] and the presence of a potassium cation coordinating to P1 [P1–K1 3.1275(6) Å] and O1 [O1–K1 2.5557(11) Å] (Fig. 5B). The nucleophilic attack to the β-P atom of **3a** aligns with the inspection of the individual atom

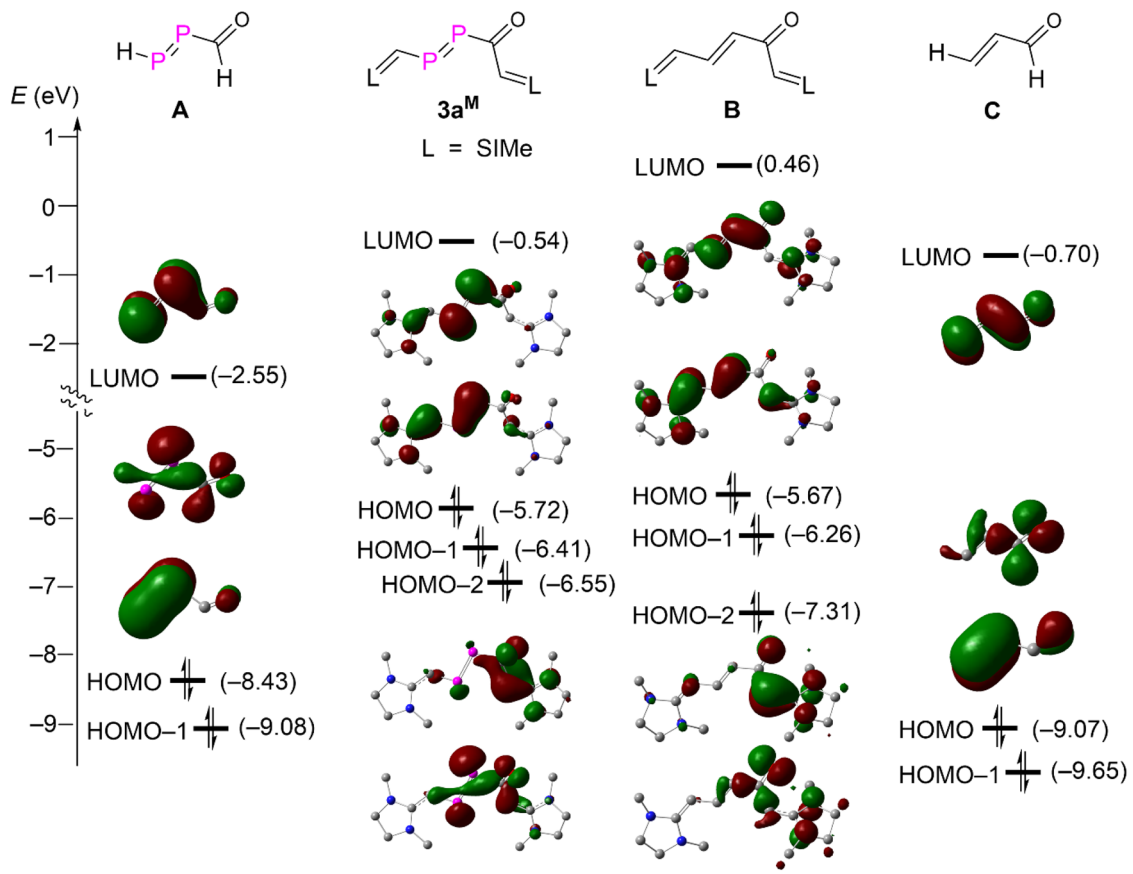

Fig. 4 Energy diagram for the frontier Kohn–Sham orbitals (isovalue = 0.04) of compound 3a^{M} and A–C.

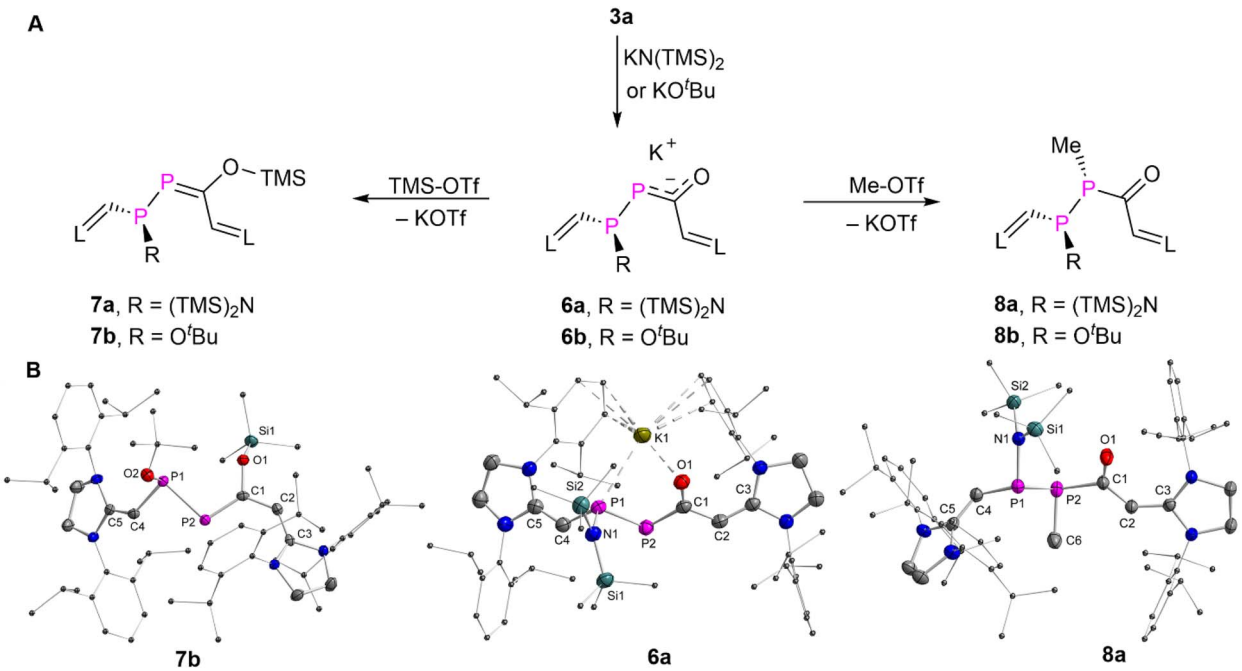

Fig. 5 (A) Synthesis of **6**–**8**. (B) Plots of the molecular structure of **6a**, **7b**, and **8a** (ellipsoids are set to 50% probability; H atoms and solvents are omitted for clarity). Selected distances (Å): **6a**: P1–K1 3.1275(6), O1–K1 2.5557(11), P1–N1 1.7716(13), P1–P2 2.1923(6), P2–C1 1.8058(17), C1–O1 1.2705(19), C1–C2 1.469(2), C2–C3 1.360(2), P1–C4 1.7957(17), C4–C5 1.352(2); **7b**: P1–O2 1.6834(13), O1–Si1 1.6593(13), P1–P2 2.2243(7), P2–C1 1.7203(19), C1–O1 1.390(2), C1–C2 1.430(3), C2–C3 1.370(3), P1–C4 1.7903(19), C4–C5 1.353(3); **8a**: P1–N1 1.739(3), P2–C6 1.862(3), P1–P2 2.2367(10), P2–C1 1.891(3), C1–O1 1.229(4), C1–C2 1.424(4), C2–C3 1.384(4), P1–C4 1.797(3), C4–C5 1.363(4).

contributions to the frontier MOs in $\mathbf{3a}^{\mathbf{M}}$ (Fig. 4). The negative charge is delocalized over the P–C–O fragment as indicated by the lengths of the P2–C1 bond [1.8058(17) Å] and C1–O1 bond [1.2705(19) Å], which are in between the P=C and C–O bonds in **7b** [1.7203(19) Å; 1.390(2) Å] and P–C and C=O bonds in **8a** [1.891(3) Å; 1.229(4) Å]. The P1–P2 [2.1923(6) Å] bond in **6a** is significantly longer than that in **3a** [2.0609(7) Å]. The P1–C4 [1.7957(17)] and C1–C2 [1.469(2)] bonds are elongated, while the C2=C3 [1.360(2)] and C4=C5 [1.352(2)] bonds are shortened as compared to those in **3a**. These data indicate a less delocalized π-electron system in **6a**.

The oxygen atom of the carbonyl group of a α-PE shows a higher affinity for a silyl group than the phosphorus atom.[5e] In order to investigate whether this accounts also for DPEs, **6a** or **6b** were treated with trimethylsilyl triflate (TMS-OTf), and the products **7a** or **7b** were isolated as yellow powders in 36% or orange powders in 52% yield (spectroscopic yield >90%, see Fig. S47 and S68†), respectively (Fig. 5A). Single crystals of **7b** suitable for XRD analysis were obtained from a saturated acetonitrile solution stored at −30 °C. XRD studies revealed that the TMS group is bound to the O1 atom [O1–Si1 1.6593(13) Å]. The C1–O1 [1.390(2) Å] bond in **7b** corresponds to a typical single bond length. The P2=C1 [1.7203(19) Å] bond is shorter than the one observed in **3a** [1.874(19) Å] and **6a** [1.8058(17) Å], and is best regarded as a double bond. Thus, **7a,b** are the products of the stepwise nucleophilic and electrophilic 1,4-addition reactions.

Alternatively, **6a** or **6b** can be reacted with methyl triflate (Me-OTf) to afford yellow powders **8a** or **8b** in 49% or 57% yield (spectroscopic yield >70%, see Fig. S53 and S75†). Multinuclear NMR spectra analyses and XRD studies confirmed that the methyl group is bonded to the P2 rather than the O1, resulting in **8a,b** as the 1,2-addition product (Fig. 4B) Note that the reaction of **6a** with triflic acid (H-OTf) yielded a mixture of unidentified products. But we could observe the formation of a protonated product with a P2–H group in solution after reaction with triethylamine hydrochloride (Et_3NHCl), which decomposed upon attempted isolation (Fig. S60 and S61†). Thus, **3a** exhibits also the reactivity of typical diphosphenes,[3h,15b] and the nucleophilic 1,2-addition reaction across the carbonyl group was not observed.

Stepwise electrophilic and nucleophilic 1,4-addition (P,O) of 3a

To probe the electrophilic 1,4-addition reactivity of **3a**, we reacted **3a** with Me-OTf and TMS-OTf yielding product **9a,b** as purple powders in over 90% yield (Fig. 6A), respectively. The proton-decoupled ^{31}P NMR spectra of **9a** displayed two doublets at $\delta(^{31}P) = 471.3$ and 229.7 ppm ($^1J_{PP} = 500.6$ Hz). The ^1H and ^{13}C NMR data as well as the HSQC spectrum (Fig. S84†) of **9a** confirmed the presence of one methoxyl group [$\delta(^1H) = 2.82$ ppm (s) and $\delta(^{13}C) = 59.6$ ppm (d, $^3J_{PC} = 24.4$ Hz)], and two CH moieties from two NHV groups [$\delta(^1H) = 4.85$ ppm (s), $\delta(^{13}C) = 87.9$ ppm (d, $^2J_{PC} = 15.8$ Hz); and $\delta(^1H) = 6.11$ ppm (t, $^2J_{PH} \approx {}^3J_{PH} = 14.1$ Hz), $\delta(^{13}C) = 103.9$ ppm (t, $^1J_{PH} \approx {}^2J_{PH} = 54.3$ Hz)]. The HMBC experiment of **9a** displayed correlations from the protons of the methoxyl group to the carbon of the PPCO

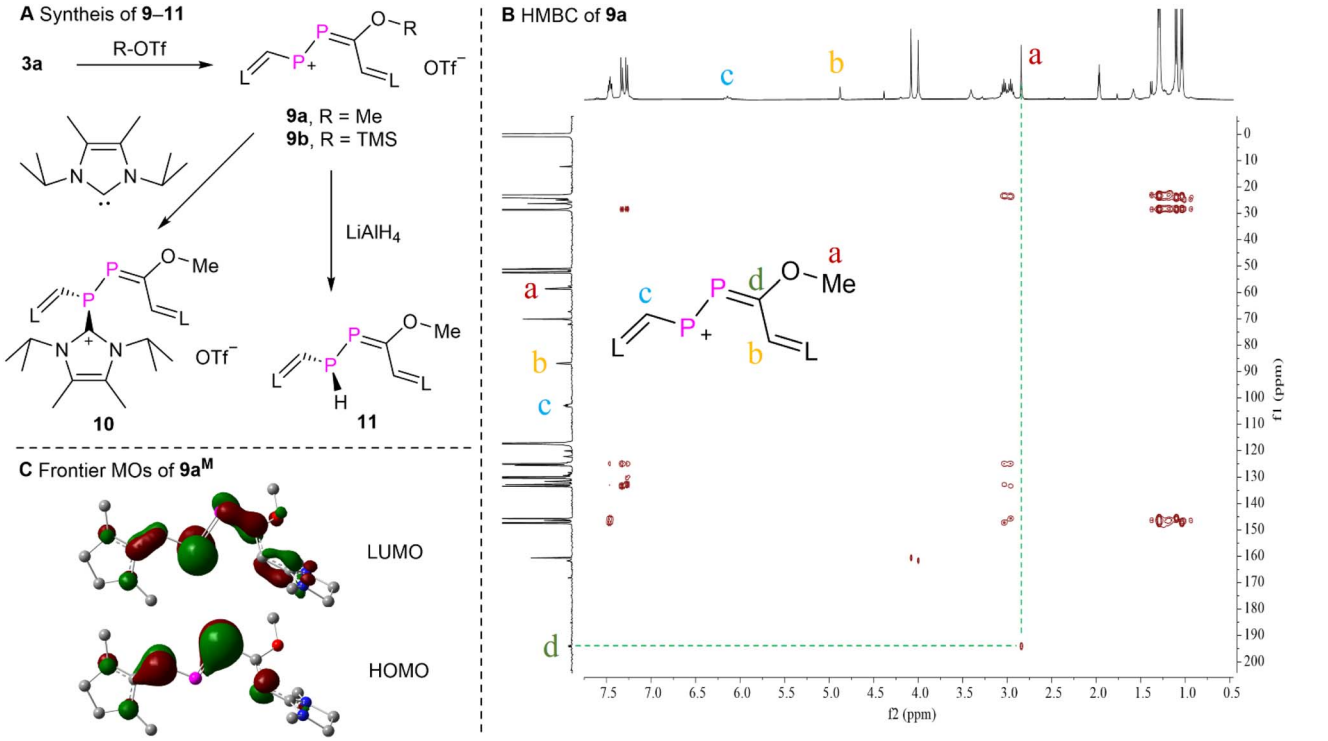

Fig. 6 (A) Synthesis of **9–11**, (B) the HMBC spectrum of **9a**, and (C) the frontier Kohn–Sham orbitals (isovalue = 0.05) of compound **9a**^{M}.

fragment, but not to the carbon nuclei of both CH moieties from the NHV groups (Fig. 6B). This assignment is in agreement with the calculated chemical shifts (Table S3†). The solution of **9a** in acetonitrile is purple and exhibits a strong absorption at λ_{max} = 569 nm (4.1 × 10^4 M^{-1} cm^{-1}). According to TD-DFT calculations this absorption corresponds to the electronic transition from the HOMO to the LUMO of **9a** (546 nm). Compound **9b** exhibits similar spectroscopic feature to those observed for **9a**. The reaction of **3a** and H-OTf also led to a product [$\delta(^{31}P)$ = 504.3 and 250.3 ppm ($^{1}J_{PP}$ = 492.8 Hz)], which was too unstable to be isolated (Fig. S100†). Thus, **3a** reacts with electrophiles under attack of the carbonyl oxygen center in line with the predicted NPA charges of the P=P–C=O fragment of **3a**^{M}, where only the oxygen atom is negatively charged (−0.64*e*, Fig. 3B).

The MOs of **9a**^{M} were calculated at the M062X/Def2SVP level of theory and reveal that the HOMO is primarily the π-type lone-pair localized on one of the phosphorus atoms adjacent to the methoxyl group with a minor contribution from two terminal NHV substituents. The LUMO is mainly the π*-type long-pair centered at the other phosphorus atom with small contributions from π*-type orbitals of the P=C bond and two NHV groups (Fig. 6C). And the NPA charges of the central P–P=C moiety of **9a**^{M} are +0.43*e*, +0.03*e*, and +0.15*e*, respectively. These MO analyses and NBO calculations unveil that the phosphorus atom adjacent to one of the NHV groups is more susceptible to nucleophilic attack. Consequently, **9a** was reacted with nucleophiles such as 4,5-dimethyl-1,3-diisopropylimidazol-2-ylidene[22] and lithium aluminium hydride ($LiAlH_4$). These reactions afforded products **10** and **11** as dark red powder or yellow oil, respectively, in over 60% yield. The relatively small J_{PP} coupling constants of **10** [$\delta(^{31}P)$ = 35.0 and −54.1 ppm ($^{1}J_{PP}$ = 265.2 Hz)] and **11** [$\delta(^{31}P)$ = 49.6 (d) and −105.9 ppm (dd, $^{1}J_{PP}$ = 221.2 Hz, $^{1}J_{PH}$ = 180.7 Hz)] indicates the diminished double bond character between two phosphorus atoms. According to calculated chemical shifts (Table S3†), the phosphorus atom (predicted to be −100.0 ppm) with a P–H bond is situated in β-position of the

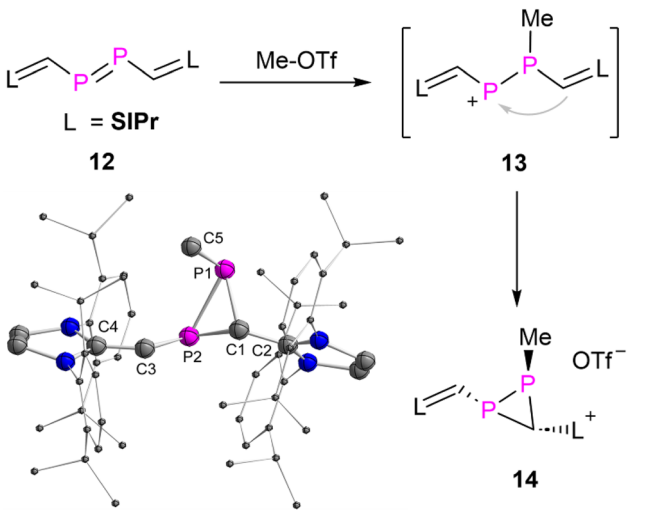

Fig. 7 Synthesis of **14** and the plot of its molecular structure (ellipsoids are set to 50% probability; H atoms, anion and solvents are omitted for clarity). Selected distances (Å): P1–P2 2.2463(7), P1–C1 1.900(2), P1–C5 1.845(2), P2–C1 1.8625(19), P2–C3 1.777(2), C3–C4 1.373(3), C1–C2 1.455(2).

C–OMe groups of **11**. Further purification of the oil **11** was not possible in our hands because of its high air sensitivity. The ^{13}C NMR spectrum of **10** displayed a characteristic doublet at $\delta(^{13}C) = 152.8$ ppm (d, $^{1}J_{PC} = 80.8$ Hz), indicating the presence of a P–C bond in which the C_2 nucleus of an NHC participates.[23] These results suggest that **10** and **11** are the products of the electrophilic conjugated 1,4-addition reaction (Fig. 6).

To differentiate the electrophilic reactivity of **3a** from diphosphenes, the diphosphene **12**,[14d] that has the same framework of **3a** except the carbonyl group, was selected to react with Me-OTf. As result product **14** was obtained as yellow powder in 91% yield (Fig. 7). Multiple NMR spectroscopic analyses and XRD study unambiguously confirmed that **14** is a three-membered heterocyclic diphosphirane. The formation of **14** proceeds likely *via* an intramolecular rearrangement *via* the hypothetical intermediate **13**, which is formed by initial electrophilic attack of a methyl cation to one of the phosphorus atoms of **12**. In contrast, the cyclic alkyl amino carbene (CAAC) substituted diphosphene showed different reactivity with Me-OTf.[24]

Conclusions

Over nearly three decades after the first syntheses and isolation of α-PE[5] and β-Pes,[6,7] this work demonstrates that the acyclic DPEs **3a,b** [NHV–P=P–C(O)–NHV] can be obtained and isolated. These novel DPEs show structural features analogous to those observed in enones. However, the replacement of both CR moieties by P atoms in enones also alter profoundly their electronic structures. Experimentally, **3a** exhibits not only 1,4-addition, but also nucleophilic 1,2-addition across the P=P bond instead of the C=O double bond. We show here that our previously established synthetic method for the preparation of transient DPEs can be generalized for the synthesis of stable DPEs *via* an intramolecular rearrangement reaction from transient phosphanyl phosphaketenes.[10] Given the variety of synthetically accessible N-heterocyclic olefines[14] and carbenes,[25] the synthetic method applied here may intrigue the preparation of previously inaccessible DPEs and other related derivatives.

Data availability

All the characterization data are available from the electronic ESI.†

Author contributions

J. Lin carried out most of the experimental work. S. Liu and S. Zheng assisted with the NMR spectra and X-ray single crystallographic diffraction measurements. Z. Li carried out the computational studies. The manuscript was written through contributions of all authors. All authors have given approval to the final version of the manuscript.

Conflicts of interest

There are no conflicts to declare.

Acknowledgements

This work was supported by the National Natural Science Foundation of China (22271315, 22171291, 21821003, 21890380), Guangdong Basic and Applied Basic Research Foundation (2021A1515012028, 2023A1515010092), Science and Technology Planning Project of Guangzhou (202102080189), National Key Research and Development Program of China (2021YFA1500401). We thank Dr Long Jiang from the Instrumental Analysis & Research Center of Sun Yat-Sen University for assistance with the SC-XRD analyses.

Notes and references

1 (*a*) J. Li, Z. Lu and L. L. Liu, *J. Am. Chem. Soc.*, 2022, **144**, 23691–23697; (*b*) F. Mathey, *Angew. Chem., Int. Ed.*, 2003, **42**, 1578–1604; (*c*) S. Wang, J. D. Sears, C. E. Moore, A. L. Rheingold, M. L. Neidig and J. S. Figueroa, *Science*, 2022, **375**, 1393–1397; (*d*) G. Rayner-Canham, *Found. Chem.*, 2011, **13**, 121–129; (*e*) E. A. LaPierre, B. O. Patrick and I. Manners, *J. Am. Chem. Soc.*, 2024, **146**, 6326–6335; (*f*) E. A. LaPierre, B. O. Patrick and I. Manners, *J. Am. Chem. Soc.*, 2023, **145**, 7107–7112; (*g*) K. B. Dillon, F. Mathey and J. F. Nixon, *Phosphorus: The Carbon Copy: From Organophosphorus to Phospha-organic Chemistry*, Wiley, 1998.

2 (*a*) G. Märkl, *Angew. Chem., Int. Ed. Engl.*, 1966, **5**, 846–847; (*b*) G. Recker, *Z. Anorg. Allg. Chem.*, 1976, **423**, 242–254; (*c*) G. Becker, G. Gresser and W. Uhl, *Z. Naturforsch., B*, 1981, **36**, 16–19; (*d*) M. Yoshifuji, I. Shima, N. Inamoto, K. Hirotsu and T. Higuchi, *J. Am. Chem. Soc.*, 1981, **103**, 4587–4589; (*e*) K. B. Dillon, V. C. Gibson and L. J. Sequeira, *J. Chem. Soc., Chem. Commun.*, 1995, 2429–2430.

3 (*a*) S. P, N. Gautam, S. Maji, K. Bhattacharyya and S. K. Mandal, *J. Am. Chem. Soc.*, 2024, **146**, 16743–16752; (*b*) Q. Luo, T. Liu, L. Huang, C. Yang and W. Lu, *Angew. Chem., Int. Ed.*, 2024, e202405122; (*c*) L. L. Liu, J. Zhou, R. Andrews and D. W. Stephan, *J. Am. Chem. Soc.*, 2018, **140**, 7466–7470; (*d*) T. G. Saint-Denis, T. A. Wheeler, Q. Chen, G. Balázs, N. S. Settineri, M. Scheer and T. D. Tilley, *J. Am. Chem. Soc.*, 2024, **146**, 4369–4374; (*e*) Y. Chen, P. Su, D. Wang, Z. Ke and G. Tan, *Nat. Commun.*, 2024, **15**, 4579; (*f*) N. T. Coles, A. Sofie Abels, J. Leitl, R. Wolf, H. Grützmacher and C. Müller, *Coord. Chem. Rev.*, 2021, **433**, 213729; (*g*) T. Görlich, P. Coburger, E. S. Yang, J. M. Goicoechea, H. Grützmacher and C. Müller, *Angew. Chem., Int. Ed.*, 2023, **62**, e202217749; (*h*) L. Weber, F. Ebeler and R. S. Ghadwal, *Coord. Chem. Rev.*, 2022, **461**, 214499; (*i*) A. Chirila, R. Wolf, J. Chris Slootweg and K. Lammertsma, *Coord. Chem. Rev.*, 2014, **270–271**, 57–74; (*j*) T. Baumgartner and R. Réau, *Chem. Rev.*, 2006, **106**, 4681–4727.

4 (*a*) L. V. R. Reddy, V. Kumar, R. Sagar and A. K. Shaw, *Chem. Rev.*, 2013, **113**, 3605–3631; (*b*) C. Brenninger, J. D. Jolliffe and T. Bach, *Angew. Chem., Int. Ed.*, 2018, **57**, 14338–14349; (*c*) G. Desimoni, G. Faita and P. Quadrelli, *Chem. Rev.*, 2018, **118**, 2080–2248; (*d*) S. Zhang, H. Neumann and M. Beller, *Chem. Soc. Rev.*, 2020, **49**, 3187–3210.

5 (*a*) E. P. O. Fuchs, H. Heydt, M. Regitz, W. W. Schoeller and T. Busch, *Tetrahedron Lett.*, 1989, **30**, 5111–5114; (*b*) E. Fuchs, B. Breit, H. Heydt, M. Regitz, W. Schoeller, T. Busch, C. Krüger and P. Betz, *Chem. Ber.*, 1991, **124**, 2843–2855; (*c*) J. Grobe, D. L. Van and G. Lange, *Z. Naturforsch., B*, 1993, **48**, 58–67; (*d*) L. Weber, S. Uthmann, H. Bögge, A. Müller, H.-G. Stammler and B. Neumann, *Organometallics*, 1998, **17**, 3593–3598; (*e*) L. Weber, S. Uthmann, H.-G. Stammler, B. Neumann, W. W. Schoeller, R. Boese and D. Bläser, *Eur. J. Inorg. Chem.*, 1999, **1999**, 2369–2381; (*f*) L. Weber, *Eur. J. Inorg. Chem.*, 2000, **2000**, 2425–2441; (*g*) L. Weber, G. Noveski, S. Uthmann, H.-G. Stammler and B. Neumann, *Eur. J. Inorg. Chem.*, 2007, **2007**, 4011–4016; (*h*) A. S. Ionkin, Y. Wang, W. J. Marshall and V. A. Petrov, *J. Organomet. Chem.*, 2007, **692**, 4809–4827; (*i*) G. Becker, M. Schmidt, W. Schwarz and M. Westerhausen, *Z. Anorg. Allg. Chem.*, 1992, **608**, 33–42; (*j*) G. Becker, M. Birkhahn, W. Massa and W. Uhl, *Angew. Chem., Int. Ed. Engl.*, 1980, **19**, 741–742.

6 (*a*) M. V. D. Sluis, F. Bickelhaupt, N. Veldman, H. Kooijman, A. L. Spek, W. Eisfeld and M. Regitz, *Chem. Ber.*, 1995, **128**, 465–476; (*b*) M. Van Der Sluis, J. B. M. Wit and F. Bickelhaupt, *Phosphorus, Sulfur Silicon Relat. Elem.*, 1996, **109**, 585–588.

7 (*a*) M. Yoshifuji, S. Ito, K. Toyota and M. Yasunami, *Bull. Chem. Soc. Jpn.*, 1995, **68**, 1206–1212; (*b*) D. Ghereg, E. André, H. Gornitzka, J. Escudié, F. Ouhsaine, N. Saffon, K. Miqueu and J.-M. Sotiropoulos, *Chem.–Eur. J.*, 2011, **17**, 12763–12772; (*c*) M. Yoshifuji, Y. Ichikawa and K. Toyota, *Tetrahedron Lett.*, 1997, **38**, 1585–1588; (*d*) M. Helena, A. Benvenutti, P. B. Hitchcock, J. L. Kiplinger, J. F. Nixon and T. G. Richmond, *Chem. Commun.*, 1997, 1539–1540; (*e*) M. Scheer and J. Krug, *Z. Anorg. Allg. Chem.*, 1998, **624**, 399–405.

8 (*a*) M. Ghalib, B. Niaz, P. G. Jones and J. W. Heinicke, *Tetrahedron Lett.*, 2012, **53**, 5012–5014; (*b*) B. R. Aluri, M. K. Kindermann, P. G. Jones and J. Heinicke, *Chem.–Eur. J.*, 2008, **14**, 4328–4335; (*c*) N. Gupta, C. B. Jain, J. Heinicke, N. Bharatiya, R. K. Bansal and P. G. Jones, *Heteroat. Chem.*, 1998, **9**, 333–339; (*d*) X. Chen, S. Alidori, F. F. Puschmann, G. Santiso-Quinones, Z. Benkő, Z. Li, G. Becker, H.-F. Grützmacher and H. Grützmacher, *Angew. Chem., Int. Ed.*, 2014, **53**, 1641–1645; (*e*) X. Chen, W. Chen, T. Ren and J. D. Protasiewicz, *Tetrahedron Lett.*, 2005, **46**, 5941–5944.

9 Z. Li, X. Chen, M. Bergeler, M. Reiher, C.-Y. Su and H. Grützmacher, *Dalton Trans.*, 2015, **44**, 6431–6438.

10 J. E. Borger, G. Le Corre, Y. Mei, R. Suter, E. Schrader and H. Grützmacher, *Chem.–Eur. J.*, 2019, **25**, 3957–3962.

11 R. J. Gilliard, R. Suter, E. Schrader, Z. Benkő, A. L. Rheingold, H. Grützmacher and J. D. Protasiewicz, *Chem. Commun.*, 2017, **53**, 12325–12328.

12 (*a*) G. Becker, W. Schwarz, N. Seidler and M. Westerhausen, *Z. Anorg. Allg. Chem.*, 1992, **612**, 72–82; (*b*) F. F. Puschmann, D. Stein, D. Heift, C. Hendriksen, Z. A. Gal, H.-F. Grützmacher and H. Grützmacher, *Angew. Chem., Int. Ed.*, 2011, **50**, 8420–8423; (*c*) A. R. Jupp and J. M. Goicoechea, *Angew. Chem., Int. Ed.*, 2013, **52**, 10064–10067; (*d*) D. Heift, Z. Benkő and H. Grützmacher, *Dalton Trans.*, 2014, **43**, 831–840; (*e*) I. Krummenacher and C. C. Cummins, *Polyhedron*, 2012, **32**, 10–13.

13 (*a*) M. M. D. Roy and E. Rivard, *Acc. Chem. Res.*, 2017, **50**, 2017–2025; (*b*) R. S. Ghadwal, *Acc. Chem. Res.*, 2022, **55**, 457–470; (*c*) C. E. I. Knappke, J. M. Neudörfl and A. J. von Wangelin, *Org. Biomol. Chem.*, 2010, **8**, 1695–1705.

14 (*a*) I. C. Watson, A. Schumann, H. Yu, E. C. Davy, R. McDonald, M. J. Ferguson, C. Hering-Junghans and E. Rivard, *Chem.–Eur. J.*, 2019, **25**, 9678–9690; (*b*) C. Hering-Junghans, P. Andreiuk, M. J. Ferguson, R. McDonald and E. Rivard, *Angew. Chem., Int. Ed.*, 2017, **56**, 6272–6275; (*c*) D. Rottschäfer, M. K. Sharma, B. Neumann, H.-G. Stammler, D. M. Andrada and R. S. Ghadwal, *Chem.–Eur. J.*, 2019, **25**, 8127–8134; (*d*) J. Lin, S. Liu, J. Zhang, H. Grützmacher, C.-Y. Su and Z. Li, *Chem. Sci.*, 2023, **14**, 10944–10952; (*e*) O. Back, B. Donnadieu, M. von Hopffgarten, S. Klein, R. Tonner, G. Frenking and G. Bertrand, *Chem. Sci.*, 2011, **2**, 858–861; (*f*) F. Dielmann, O. Back, M. Henry-Ellinger, P. Jerabek, G. Frenking and G. Bertrand, *Science*, 2012, **337**, 1526–1528; (*g*) A. J. Arduengo, F. Davidson, H. V. R. Dias, J. R. Goerlich, D. Khasnis, W. J. Marshall and T. K. Prakasha, *J. Am. Chem. Soc.*, 1997, **119**, 12742–12749; (*h*) H. Klöcker, M. Layh, A. Hepp and W. Uhl, *Dalton Trans.*, 2016, **45**, 2031–2043.

15 (*a*) M. Yoshifuji, *Eur. J. Inorg. Chem.*, 2016, **2016**, 607–615; (*b*) L. Weber, *Chem. Rev.*, 1992, **92**, 1839–1906.

16 (*a*) P. Pyykkö and M. Atsumi, *Chem.–Eur. J.*, 2009, **15**, 12770–12779; (*b*) F. H. Allen, O. Kennard, D. G. Watson, L. Brammer, A. G. Orpen and R. Taylor, *J. Chem. Soc., Perkin Trans. 2*, 1987, S1–S19.

17 (*a*) Q. Shen, J. Xu and X. Chen, *Dalton Trans.*, 2022, **51**, 10240–10248; (*b*) A. C. Tsipis, *Organometallics*, 2006, **25**, 2774–2781.

18 E. D. Glendening, J. K. Badenhoop, A. E. Reed, J. E. Carpenter, J. A. Bohmann, C. M. Morales, P. Karafiloglou, C. R. Landis and F. Weinhold, *NBO 7.0*, 2018.

19 S. Patchkovskii and T. Ziegler, *J. Phys. Chem. A*, 2002, **106**, 1088–1099.

20 (*a*) M. M. Hansmann, D. A. Ruiz, L. L. Liu, R. Jazzar and G. Bertrand, *Chem. Sci.*, 2017, **8**, 3720–3725; (*b*) Z. Li, X. Chen, Z. Benkő, L. L. Liu, D. A. Ruiz, J. L. Peltier, G. Bertrand, C.-Y. Su and H. Grützmacher, *Angew. Chem., Int. Ed.*, 2016, **55**, 6018–6022; (*c*) L. Liu, D. A. Ruiz, D. Munz and G. Bertrand, *Chem*, 2016, **1**, 147–153; (*d*) J. M. Goicoechea and H. Grützmacher, *Angew. Chem., Int. Ed.*, 2018, **57**, 16968–16994; (*e*) D. W. N. Wilson, J. Feld and J. M. Goicoechea, *Angew. Chem., Int. Ed.*, 2020, **59**, 20914–20918.

21 (*a*) M. J. Frisch and *et al.*, *Gaussian 16*, Revision C.01, 2016; (*b*) A. Bondi, *J. Phys. Chem.*, 1964, **68**, 441–451.

22 N. Kuhn and T. Kratz, *Synthesis*, 1993, **1993**, 561–562.

23 (*a*) Z. Li, X. Chen, Y. Li, C.-Y. Su and H. Grützmacher, *Chem. Commun.*, 2016, **52**, 11343–11346; (*b*) D. Dhara, P. Kalita, S. Mondal, R. S. Narayanan, K. R. Mote, V. Huch, M. Zimmer, C. B. Yildiz, D. Scheschkewitz, V. Chandrasekhar and A. Jana, *Chem. Sci.*, 2018, **9**, 4235–

4243; (*c*) M. Balmer, H. Gottschling and C. von Hänisch, *Chem. Commun.*, 2018, **54**, 2659–2661; (*d*) H. Chen, Y. Chen, T. Li, D. Wang, L. Xu and G. Tan, *Inorg. Chem.*, 2023, **62**, 20906–20912; (*e*) M. M. Hansmann and G. Bertrand, *J. Am. Chem. Soc.*, 2016, **138**, 15885–15888; (*f*) J. E. Walley, L. S. Warring, E. Kertész, G. Wang, D. A. Dickie, Z. Benkő and R. J. Gilliard Jr, *Inorg. Chem.*, 2021, **60**, 4733–4743; (*g*) A. Doddi, D. Bockfeld, T. Bannenberg, P. G. Jones and M. Tamm, *Angew. Chem., Int. Ed.*, 2014, **53**, 13568–13572; (*h*) A. M. Tondreau, Z. Benkő, J. R. Harmer and H. Grützmacher, *Chem. Sci.*, 2014, **5**, 1545–1554; (*i*) M. K. Sharma, S. Chabbra, C. Wölper, H. M. Weinert, E. J. Reijerse, A. Schnegg and S. Schulz, *Chem. Sci.*, 2022, 12643–12650.

24 L. L. Liu, L. L. Cao, J. Zhou and D. W. Stephan, *Angew. Chem., Int. Ed.*, 2019, **58**, 273–277.

25 (*a*) D. Martin, M. Soleilhavoup and G. Bertrand, *Chem. Sci.*, 2011, **2**, 389–399; (*b*) C. D. Martin, M. Soleilhavoup and G. Bertrand, *Chem. Sci.*, 2013, **4**, 3020–3030; (*c*) M. N. Hopkinson, C. Richter, M. Schedler and F. Glorius, *Nature*, 2014, **510**, 485–496; (*d*) P. Bellotti, M. Koy, M. N. Hopkinson and F. Glorius, *Nat. Rev. Chem*, 2021, **5**, 711–725; (*e*) A. Doddi, M. Peters and M. Tamm, *Chem. Rev.*, 2019, **119**, 6994–7112; (*f*) V. Nesterov, D. Reiter, P. Bag, P. Frisch, R. Holzner, A. Porzelt and S. Inoue, *Chem. Rev.*, 2018, **118**, 9678–9842; (*g*) M. Melaimi, R. Jazzar, M. Soleilhavoup and G. Bertrand, *Angew. Chem., Int. Ed.*, 2017, **56**, 10046–10068; (*h*) M. Soleilhavoup and G. Bertrand, *Acc. Chem. Res.*, 2015, **48**, 256–266.